OPEN ACCESS

ACTA METALLURGICA SLOVACA

2026, VOL. 32, NO. 1, 41-48

RESEARCH PAPER

Optimization of cyanide detoxification in gold mine tailings using sodium percarbonate

Ainur Berkinbayeva, Shynar Saulebekkyzy, Diana Karim, Akniyet Bakkozha*

Institute of Metallurgy and Ore Beneficiation, Satbayev University, Almaty, Kazakhstan

*Corresponding author: sh.saulebekkyzy@satbayev.university, tel.: +7 747 608 01 79, Institute of Metallurgy and Ore Beneficiation, Satbayev University, Almaty, Kazakhstan

Received: 19.02.2026
Accepted: 23.02.2026

ABSTRACT

Wastewater containing cyanide, produced during gold extraction operations, poses a significant environmental threat and requires detoxification procedures that comply with rigorous regulatory standards, including those set by the International Cyanide Management Code (ICMI). Sodium percarbonate was evaluated as an oxidizing agent for the treatment of hydrometallurgical tailings contaminated with cyanide, which is formed at the Altyntau Kokshetau enterprise in Kazakhstan. The operating conditions were optimized using the response surface methodology based on the central composite design (CCD). In experiments carried out at room temperature, pH, oxidizer dose and reaction time were identified as the main factors. The composition of the waste and the transformation of cyanide were monitored using ICP-OES, FTIR spectroscopy, and spectrophotometric quantification of residual cyanide. Treatment with sodium percarbonate reduced the cyanide concentration to below the ICMI limit of 0.2 mg/L and obeyed the biphasic pseudo-first-order kinetics. Of the parameters investigated, pH exhibited the most pronounced influence; it further modulates radical stability and governs the equilibrium between HCN and CN^-. The aggregate findings demonstrate that sodium percarbonate constitutes a scalable, environmentally benign alternative to conventional methods for cyanide detoxification in gold-mining effluents.

Keywords: cyanide detoxification; sodium percarbonate; hydrometallurgical wastes; gold mining; response surface methodology

INTRODUCTION

Cyanides are characterized by the -C≡N functional group and are found in various physico – chemical forms: free ionic species, metal-cyanide coordination complexes, crystalline salts (for example, KCN), as well as volatile hydrogen cyanide (HCN) [1-2]. Entry into the environment occurs through several industrial flows; among them, the predominant share is contributed by hydrometallurgical gold mining [3], while electroplating, semiconductor manufacturing, and polymer synthesis are also significant sources [4-5]. Kazakhstan's largest gold reserves ensure the country's clear role in the mining and refining industries [6]. This resource base supports economic growth and international competitiveness; forecasts for 2026 indicate the introduction of additional capacities through heap leaching [7-8] and the expansion of cyanidation practices [9]. The mechanism of toxicological action is well described. Cyanide irreversibly inhibits cytochrome c oxidase (mitochondrial IV complex), blocks the transfer of electrons to molecular oxygen, suppresses oxidative phosphorylation and causes systemic hypoxia [10]. Damage is not limited to acute mortality. Cyanide concentrations between 0.5-3.5 mg/L have been reported to induce apoptosis in neuronal and cardiac tissues independently of the pathway of action [11]. A second, chronic source is cyanogenic glycosides in plants: lotaustraline and prunasin are characteristic representatives of this class; they can release HCN upon enzymatic hydrolysis [12]. Long-term exposure has been associated with reproductive disorders, including a decrease in sperm motility due to endocrine dysregulation, as well as a weakening of cognitive function [13].

Despite these risks, cyanide leaching remains the primary hydrometallurgical method for extracting gold [14-15]. During cyanidation, sodium cyanide converts metallic Au(0) into a stable and water-soluble $Au(CN)_2^-$ and for oxidized ores, a yield of 90-95% is usually achieved. Therefore, the environmental consequences of cyanidation in mining regions are systematically studied [16-17]. In such a situation, engineering isolation, strict operational control, and clear risk-reduction measures are mandatory; neither dilution nor natural attenuation is considered sufficient protection.

Regulatory attention is further intensified due to the apparent dependence of HCN specification and volatility on pH. since pK_a = 9.21, the volatilization rate (volatilization) increases significantly as the pH drops below 9. This pattern is reflected in the US EPA criteria: maximum allowable concentration (MCL) of 0.2 mg/L for free cyanide in drinking water [18-19], criterion maximum acute effect concentration (CMC) of 22 μg/L for fresh water, as well as criterion continuous concentrations (CCC) for chronic effect: 5.2 μg/L for fresh water and 1 μg/L for seawater. These limits are combined with data describing the hypersensitivity of aquatic organisms, as cyanide exposure is associated with oxidative stress and mitochondrial dysfunction [20].

Given the variability in tolerance thresholds across species, continuous surveillance at tailings storage facilities and discharge locations is imperative for operational reasons. Process water and effluents can destabilize aquatic ecosystems by increasing the accumulation of reactive oxygen species and disrupting energy metabolism [21]; studies in which nanocomplex-based interventions have been used have provided visual evidence that they are compatible with these stress pathways.

Concomitant with the expansion of gold production, an increase in cyanide residues in waste and process waters is anticipated, thereby rendering pre-discharge treatment mandatory. Mitigation approaches include chemical methods (chlorination [22], ozonation, hydrogen peroxide oxidation, sulfide precipitation), physico-chemical approaches (adsorption [23], membrane filtration, electrocoagulation), and biodegradation strategies [24-25]. Physico-chemical schemes often achieve high removal efficiencies; however, their implementation is constrained by capital costs, energy intensity, and maintenance burden; such constraints may shift the choice towards chemical or biological alternatives [26]. Under alkaline conditions, alkaliphilic microorganisms isolated from soda lakes offer a biological route for cyanide conversion [27]. Bacillus spp. has additionally been demonstrated to metabolize cyanide under conditions of elevated pH [28-29]. Industrial performance, however, deteriorates in the presence of heavy metals and competing anions. Alkaline chlorination using sodium hypochlorite is still considered a common traditional chemical approach: at pH 10-11 and 20-25 °C, it can oxidize the CN^- ion to the CNO^- (cyanate) form. However, this method requires strict technological control, as it is mandatory to limit the risk of cyanogen chloride formation, prevent excessive oxidizer consumption, and control the need for post-treatment pH correction [30].

The conversion of cyanide to cyanate without the formation of halogenated intermediates is realized when highly reactive particles-hydroxyl (OH) and superoxide radicals are formed in an alkaline environment. These radicals are produced in advanced oxidation processes (AOPs) involving the utilization of percarbonate in conjunction with activated periodates [32-33]. It follows from this that the radical oxidation mechanism bypasses the main limitation of hypochlorite schemes: in the case of hypochlorite participation, the reaction branches are preserved, where halogen-containing intermediates can be formed, and the radical regime structurally reduces this risk.

Against the background of these safety requirements and technological predictability, attention has naturally shifted towards oxidants with a low risk of secondary contamination [31]. In this context, sodium percarbonate is considered as a relatively safe oxidizing agent suitable for the tasks of detoxification and "reduction/neutralization" of cyanide in aqueous media. Its practical attractiveness is not related to abstract "efficiency" but to the process's controllability via pH and to the net decomposition into H2O2 and Na2CO3, which eliminates the need to introduce chlorine-containing reagents and simplifies control of secondary products [34-36]. The observed trend implies that it is precisely these properties that make percarbonate increasingly in demand in the treatment of mine and process waters as a scalable and safer alternative to chlorine oxidizers [37]. Current generalizations in the literature show that sustainable management of cyanide - containing effluents should rely on oxidative chemistry, if necessary, on catalytic intensification, and on explicit reference to the structure of ecotoxicological risks, and not only to the removal rate [38]. In this context, the data from RSM – optimized biodegradation studies provide a parallel conclusion: when wastewater composition and operational constraints are mutually "linked", multiparametric optimization becomes not a cosmetic adjustment, but an obligatory stage of process design [39].

The objective of this study is to assess sodium percarbonate as an oxidant for eco-efficient detoxification of cyanide-laden hydrometallurgical tailings from a gold-mining operation. Process variables (pH, oxidant dosage, reaction time, and temperature) were optimized by response surface methodology coupled with a central composite design to maximize cyanide removal while meeting stringent environmental requirements, including the ICMI limit of 0.2 mg/L free cyanide [40-42].

MATERIAL AND METHODS

The study focused on cyanide-rich process fluids associated with hydrometallurgical tailings. Samples were taken from the Altyntau Kokshetau gold processing enterprise in northern Kazakhstan. This facility was chosen as a leading national operation because the relatively stable characteristics of the ore and effective process control ensure that the composition of exhibits consistent composition (**Table 1**). Such chemical repeatability creates a reliable basis for the development and parameterization of the detoxification process based on sodium percarbonate. Although this work is limited to the data of this enterprise, further studies should assess the robustness for waste with different matrices, including in the case of flows rich in heavy elements or with a high cyanide load [14]. Sampling was carried out in accordance with ISO 5667-3:2018 to ensure data comparability and minimise artefacts.

The wastewater was collected in 1 L polymer containers; the containers were pre-treated and sanitized, rinsed with ultrapure water, and delivered in insulated containers at 4 °C to maintain the original specification. All samples were stored at 4 °C and analysed for 48 hours to minimise cyanide degradation and compositional drift. The scope of analysis included elements Au, As, Cu, Zn, and Ag, as well as free cyanide and thiocyanate, the main anionic species [16, 37, 39].

Table 1 Chemical Composition of the Liquid Phase of Hydrometallurgical Tailings

Chemical compounds	Au	As	Cu	Zn	Ag	CN^-_{free}	CNS^-
Concentration, mg/L	0.10	7.01	4.74	0.63	0.15	443.23	257.51

Advanced analytical methods were used to characterize the cyanide-containing liquid phase of hydrometallurgical tailings and to ensure reproducible quantification. Elemental composition was measured by ICP-OES (Optima 8300DV, PerkinElmer) using certified Merck standards; all analyses were performed in triplicate with relative errors ≤3%. Free cyanide (CN^-) and ammonium (NH_4^+) were quantified by VIS spectrophotometry (Spectroquant Prove 100, Merck) with Merck test kits detection limits were 0.01 mg/L (CN^-) and 0.02 mg/L (NH_4^+). pH and redox potential (ORP/Eh) were monitored using an ITAN pH-meter/ionometer (NPP Tom'analit). Cyanide speciation and reaction products were examined by FTIR (FT/IR-6X, JASCO) with spectral processing in Spectra Manager and functional group analysis. Detoxification was carried out as a staged workflow: 0.45 μm filtration; oxidation with sodium percarbonate ($2Na_2CO_3 \cdot 3H_2O_2$) at pH 10-12, 1.5-4.0 g oxidant, 20-25 °C, 8 h contact time, and 300 rpm stirring; and neutralization with dilute H_2SO_4 to pH 6.5-7. Experiments were conducted in 1 L polyethylene vessels. Residual cyanide was measured spectrophotometrically as above, and detoxification efficiency was calculated as $DE(_t) = (C_0 - C_t)/C_0 \times 100$. Statistical modelling and optimisation were employed using Design-Expert 25.0, using RSM with a central composite design to quantify the effects of pH, oxidant dosage, and reaction time on DE. One-factor preliminary screening (OVAT) defined the working ranges, and each CCD run was replicated at least three times to maximize DE while reducing reagent demand and treatment time. The full step chart appears in **Fig. 1**.

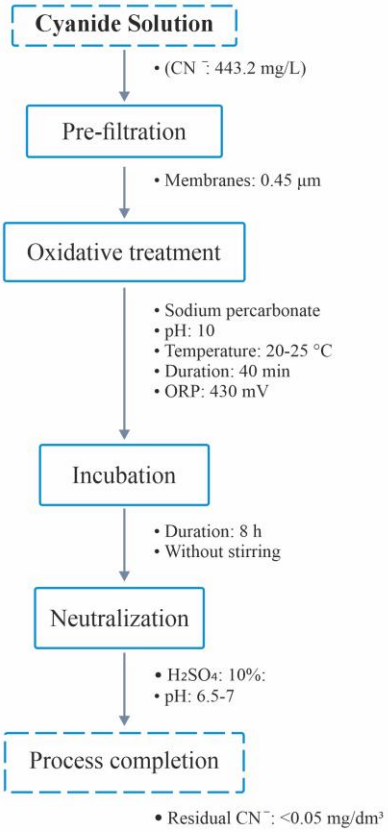

Fig. 1 Schematic flowchart of the cyanide detoxification process using sodium percarbonate

Residual toxin concentrations were measured immediately after sampling using a Spectroquant Prove 100 VIS, which provide a detection limit of 0.01 mg/L. We quantified neutralization performance as cyanide detoxification efficiency using:

$$DE(t) = (C_0 - C_t)/C_0 \times 100 \quad (1.)$$

Where: DE(t) – cyanide detoxification efficiency (%).
C_0 – initial cyanide concentration (mg/ L).
C_t – residual cyanide concentration at time (mg/L).

To describe the reaction rate, we fitted the detoxification data with a pseudo-first-order kinetic model:

$$C_t = C_0 \exp(-kt), \quad (2.)$$

Where: k – is the rate constant (min^{-1}).
t – is time (min).

Mathematical modeling and process optimization were performed in Design Expert 25.0 by combining the response surface methodology (RSM) with the central composite plan (CCD). The analysis assessed the effects of pH, sodium percarbonate dose, and oxidation time on the ECE indicator. CCD implementations were preceded by screening using the method of simultaneous change of one factor (OVAT) at Parametric intervals given in **Table 2**. This preliminary stage clarified the variables that had a dominant influence on the response and set practical working windows for the subsequent multifactorial plan. During OVAT, only one factor was changed, and the remaining parameters were kept constant under initial conditions (dose 3.5 g, time 20 min, pH 11); these basic values were selected based on the existing literature on peroxide oxidation. The screening outcomes revealed a pronounced dependency on pH, whereas the effects of dosage and duration were comparatively minor; consequently, the central points of the central composite design (CCD) were iteratively adjusted (e.g., dosage by 2.75 g, duration by 25 min) to more precisely delineate the optimum. In analogous scenarios, three experimental series were conducted (denoted by an asterisk in **Table 2**). Each test was repeated at least three times, and the average values were used in the final analysis. The aim of the optimization was to take into account reagent consumption and process duration, as well as maximizing the DE (%) value [26, 40-41].

Table 2 Detoxification parameters and experimental ranges

Parameter	Value
Concentration (g)	1.5, 2.0, 2.5, 2.75, 3.0, 3.5
Time(min)	10, 20, 30, 40
pH	10, 11, 12

In order to accurately determine the most suitable operating mode and maintain the repeatability and analytical accuracy of the data, the cyanide detoxification process was studied by combining the response surface methodology (RSM) and the central composite plan (CCD). Three independent factors were considered: the dose of sodium percarbonate (g), the processing time by oxidation (min) and the pH value of the solution. As part of this approach, RSM was used to construct a secondary polynomial equation describing the relationship between the selected process variables and the response indicator detoxification efficiency:

$$y = b_0 + \sum_{i=1}^{k} b_i x_i + \sum_{i=1}^{k} b_{ii} x_i^2 + \sum_{i=1}^{k-1} \sum_{j=i+1}^{k} b_{ij} x_i x_j \quad (3.)$$

Where: y – is the model-predicted cyanide removal efficiency.
b_0 – is the intercept.
b_i, b_{ii}, and b_{ij} – are the coefficients associated with linear, quadratic, and interaction contributions, respectively.
k – denotes the number of variables considered.

The CCD incorporated six replicated center points to estimate pure error, and we performed each experimental condition in triplicate to quantify run-to-run scatter. **Table 3** summarizes the investigated factors together with their coded levels and corresponding experimental ranges.

Table 3 Levels and codes of factors for CCD

Factors	Symbol	Coding Level		
		−1	**0**	**1**
Concentration $2Na_2CO_3 \cdot 3H_2O_2$ (g)	A	1.5	2.75	3.5
Time(min)	B	10	25	40
pH	C	10	11	12

RESULTS AND DISCUSSION

Statistical Analysis and Model Fitting.

Statistical processing and model calibration. **Table 4** summarizes the results of dispersion analysis (Anova) for the response Surface model used to describe the cyanide detoxification pathway. The explanatory capacity of the created model was assessed using the F-test; this indicator is calculated as the ratio of the share of variation explained by regression approximation to the residual variance. The fact that the F-value obtained by ANOVA is 84.50 clearly proves that the model is statistically highly significant. It is almost impossible for such an obvious F-value to be caused by random fluctuations ($p < 0.0001$). In conclusion, in the studied factor intervals – pH 10-12, sodium percarbonate content 1.5-4.0 g and reaction duration 10-40 min – The Square model reliably describes the influence of the control variables on the neutralization efficiency [37].

Table 4 Analysis of variance for the response-surface approximation of the cyanide detoxification process

Source	Sum of Squares	df	Mean Square	F Value	*p* – Value Prob > F	Standard Error	95% CI (Lower-Upper)
Model	7758.88	9	862.10	84.50	< 0.0001	-	-
A – Concentration	511.37	1	511.37	50.13	< 0.0001	±0.91	(8.56 – 12.50)
B – Time	1664.24	1	1664.24	163.13	< 0.0001	±1.64	(18.42 - 25.60)
C – pH	654.65	1	654.65	64.17	< 0.0001	±1.09	(-10.92 – -6.22)
AB Interaction	92.87	1	92.87	9.10	0.0130	±1.15	(1.12 – 6.04)
AC Interaction	333.16	1	333.16	32.66	0.0002	±1.14	(-9.18 – -4.29)
A^2 – Quadratic	77.11	1	77.11	7.56	0.0205	±3.13	(1.85 – 15.81)
C^2 – Quadratic	126.60	1	126.60	12.41	0.0055	±1.89	(2.69 – 10.96)
Residual Error	102.02	10	10.20	-	-	-	-
Cor total	7860.19	19					

Since it is based on empirical identification (fit), the model's reliability is limited only by the factorial intervals actually studied; in regions outside these limits, extrapolating the forecast is methodologically unreasonable rather than informative. An additional limitation arises from the functional type of the model: since the quadratic dependence of the response is assumed in advance, this approach may "soften" the apparent nonlinear behavior and ignore the high-order contributions often observed in complex interconnected systems [26].

Nevertheless, the quadratic model was clearly supported by a statistical test ($p < 0.0001$), that is, the matched response surface is not explained by random variation. The members that maintained the statistical weight under the traditional value limit ($p \leq 0.0500$) were A, B, C, AB, AC, A^2, and C^2. In order to personalize the variables that actually determine the answer, the full quadratic model was brought to a condensed regression form by leaving only the valued members at a confidence level of 95%. The resulting regression equation is as follows:

$$DE = 30.62 + 17.19A + 18.35B - 10.28C + 4.47AB - 8.41AC + 13.80A^2 + 6.83B^2 \quad (4.)$$

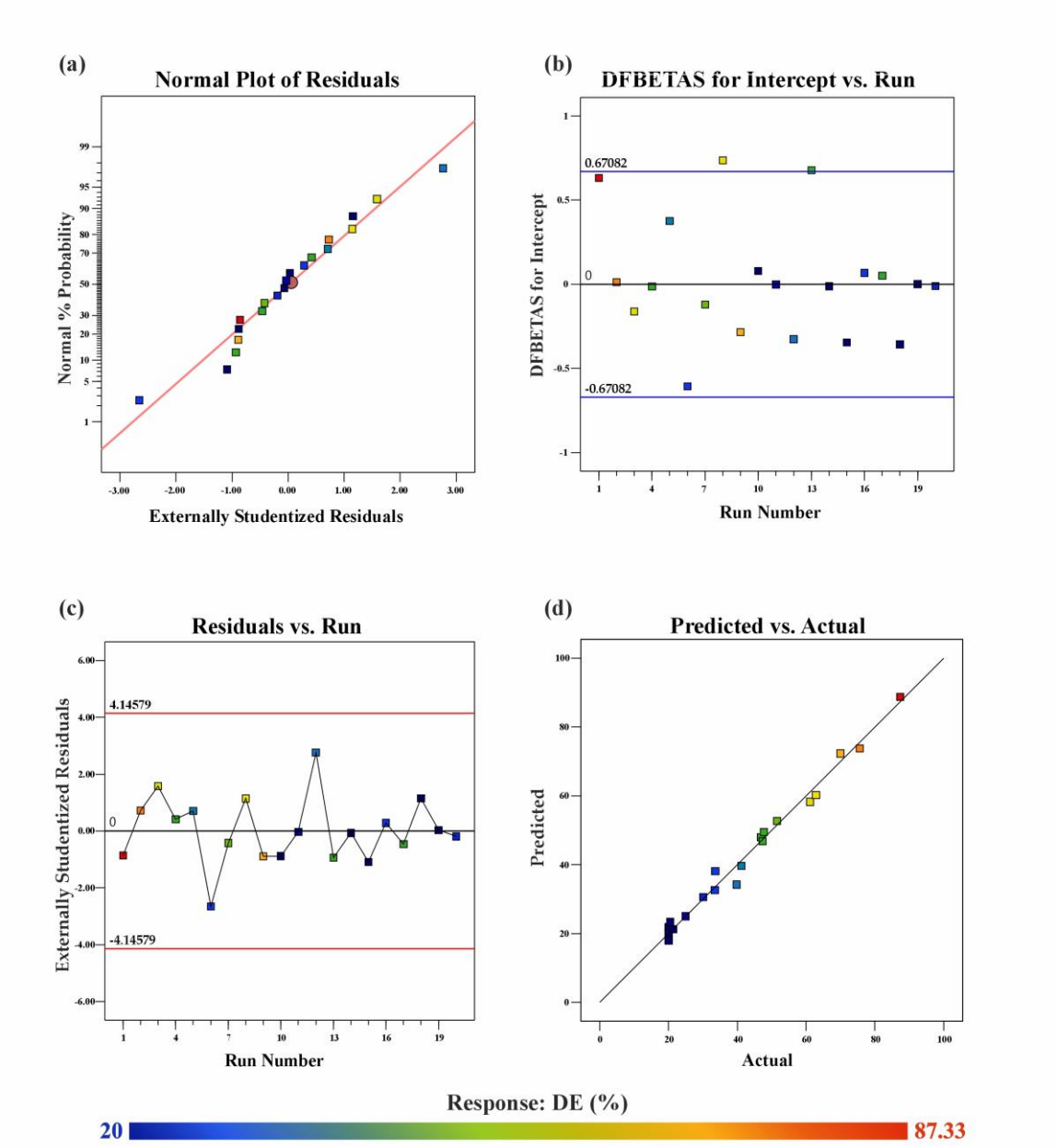

Fig. 2 Diagnostic plots for the quadratic model: (a) normal probability plot of externally studentized residuals, (b) DFBETAS for the intercept versus run number, (c) externally studentized residuals versus run number, and (d) predicted versus actual removal efficiency

Standard diagnostic graphs were analyzed to verify that the quadratic response surface describes the experimental data with sufficient accuracy. In **Fig. 2a**, the measured and predicted values are very close to the 45° match line, indicating that there are few residues (residuals) and that the results of repeat experiments are consistent. The normal probability graph of waste also supports this conclusion: waste is approximately linearly distributed, indicating that its distribution is close to normal and that there is no systematic bias.

Diagnostic procedures performed in accordance with the experimental sequence yield similar conclusions. In **Fig. 2b** and **2c**, the residues are randomly scattered along the t-Axis (-3.00 to 3.00), concentrated near zero, and a clearly structured pattern is not observed. The absence of time-dependent drift, together with the lack of increased dispersion, substantially reduces the probability of heteroscedasticity, indicating that a second-order polynomial model is sufficient to describe the effect of the operating variables on removal efficiency. On this basis, the model was assumed to be statistically stable in the studied factor space and suitable for forecasting. A parity plot presented in **Fig. 2d** demonstrates excellent agreement between the predicted values and the experimental measurements. The slope of the identification line approaches unity, and the data lie within a narrow range near that line; this confirms agreement between the calculated and observed responses and justifies using the quadratic model to assess performance under the tested conditions. After confirming the validity of the model, the proportion of the main and interacting factors affecting the efficiency of cyanide removal was analyzed: A (concentration), A (time) and C (pH).

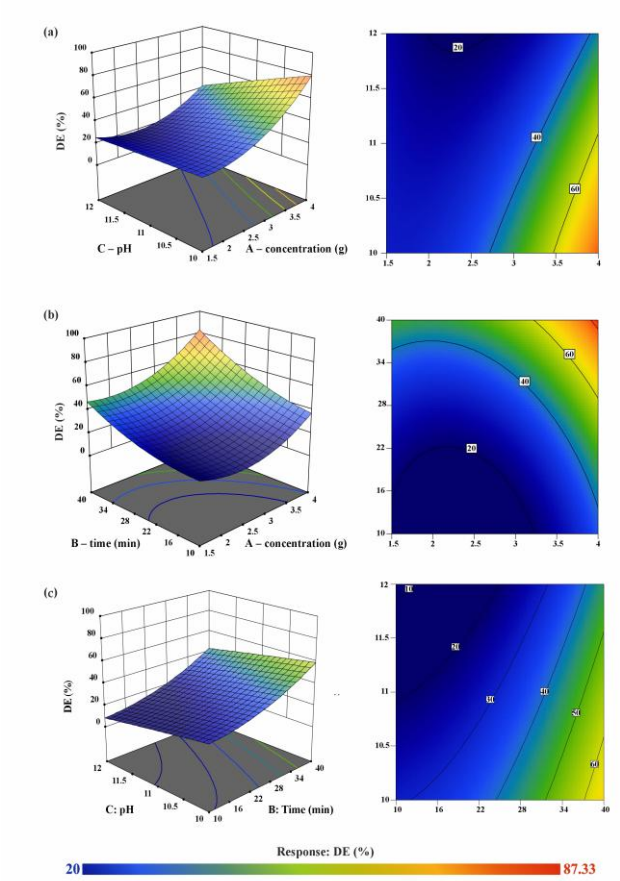

Fig. 3 Three-dimensional response surfaces and corresponding contour plots showing the coupled effects of: pH and dosage, duration and dosage, and pH and duration

Fig. 3 summarises these effects and shows how each variable and its combinations form the detoxification behaviour in the residual matrix [35]. In the fitted regression model, the estimated linear coefficients for factors A (oxidant concentration), B (reaction time), and C (pH) were 10.53, -8.57, and 22.01, respectively.These coefficients quantitatively describe in what direction and to what extent each variable changes the efficiency of removing cyanide (removal efficiency); their symbols are combined with the mechanistic expectations previously described for oxidation systems in alkaline environments [13, 30]. In the considered data set, the oxidant doze (A) and pH (C) act in the direction of increasing the cyanide removal efficiency, while the time term (B) is enters with a negative sign. Such a sign pattern suggests to the non-monotonic nature of kinetics, that is, the dependence is not limited to the simple principle that removal increases with time. A comparative assessment of the influence of factors on the response gives the series C (pH) > a (dose) > B (time). This hierarchy is chemically based: the alkaline medium favors radical-mediated oxidation, resulting in accelerated cyanide conversion channels [34]. The negative coefficient with respect to time is explained by the gradual depletion of the oxidizer and the transition to modes limited by mass transport and the turnover of intermediates after the consumption of the easily oxidized cyanide fraction. Increasing the sodium percarbonate dose has the opposite effect: it increases the available oxidative potential and ensures that transformations continue along the target reaction chain.

These interdependent effects are evident in the three-dimensional response surfaces derived from the quadratic model. A-C interactions indicate that increasing the dose or pH increases the detoxification efficiency; however, in the area of higher doses, the additional increase slows down and the surface becomes flatter and closer to the plateau. This phenomenon corresponds to the formation of a mode in which the "diminishing returns" when the concentration approaches the upper limit. Contour maps also confirm the same control logic: pH remains the main control lever; in the low–to-medium area, the response gradient increases sharply, consistent with pH-governed kinetics.

A-B projections describe the joint effect of dose and time in the studied factor space. Increasing both factors improves the response, and the geometry of the contours shows a clearer gradient along the time axis; this confirms that sensitivity to time is measurable under the given conditions.

In contrast, B-C surfaces show pH dominance: as the pH increases (about 10-12), the slopes increase, and the effect becomes more pronounced at longer reaction times. Most importantly, even at short processing intervals (≈10-25 min), the optimal pH mode increases efficiency, which once again proves the controlling role of pH.

In general, the results of the Model point to pH as the main factor determining the efficiency of removal; it is followed by the dose of oxidizer, and the proportion of time is expressed in a relatively weak and non-monotonous nature. The same hierarchy (pH > concentration > time) is also supported by F-statistics and regression coefficients. The interaction effects are limited to bounded regions of factor space, which makes it possible to predict optimal working conditions compatible with the response surfaces in **Fig. 3**.

As a result of the optimization based on the model, a concentration of 3.5 g, a working Point corresponding to a pH of 10 and a reaction time of 40 min were obtained; the detoxification efficiency predicted under these conditions was 87.2% (desirability=0.98). Validation experiments showed a value of 87.33%, indicating a high degree of agreement between the forecast and measurement and the adequacy of the matched model**.**

Kinetics and Long-Term Detoxification Performance

Cyanide breakdown in hydrometallurgical tailings' water displays a two-stage pattern: an swift early phase followed by a slower diffusion-constrained period. Beginning at 443.2 mg/L, the initial 40 minutes yield 83.33% removal efficiency, dropping levels to≈73.77 mg/L at a pseudo-first-order rate $k_1 = 0.0517$ min^{-1} with optimal settings (pH 10, 3.5 g sodium percarbonate). Extended monitoring shows 99.99% RE after 8 hours, reducing to 0.05 mg/L under a secondary rate $k_2 = 0.01665$ min^{-1}. Midpoint values match models: 19.48 mg/L at 2 hours, 2.63 mg/L at 4 hours, and 0.38 mg/L at 6 hours.

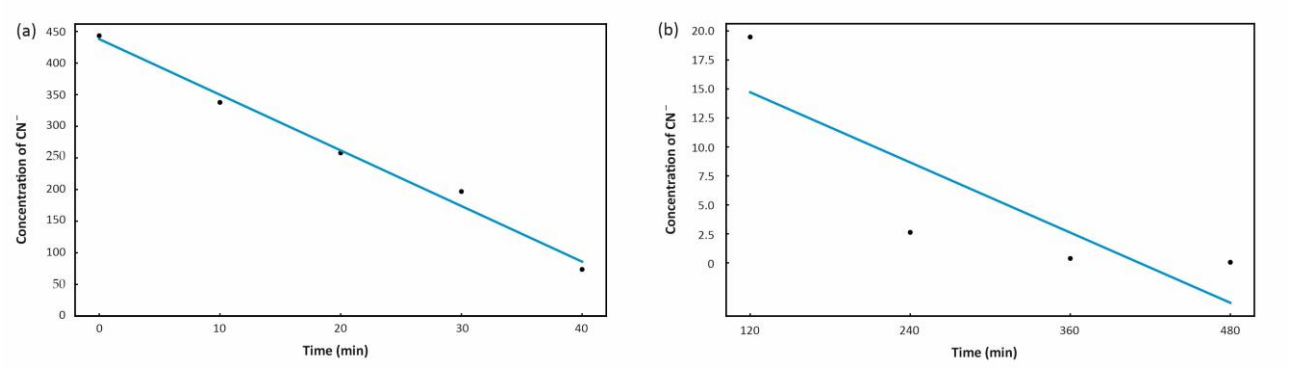

Fig. 4. a) Concentration profile of CN^- from 0 to 40 minutes; b) Concentration profile of CN^- from 120 to 480 minutes

To further elucidate the pronounced pH dependency observed in these biphasic kinetic profiles (as depicted in **Fig. 4**, where the initial rapid phase transitions into a slower diffusion-limited stage, and to justify the strategic preference for alkaline conditions in enhancing the efficiency of radical-mediated oxidation processes, a simplified Pourbaix (Eh-pH) diagram for the $HCN/CN^-/CNO^-$ system is presented in **Fig. 5**.

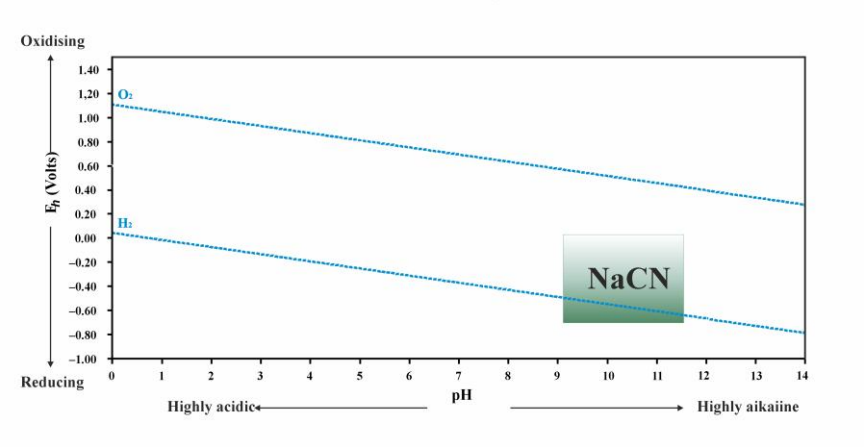

Fig. 5 Potential-pH diagram showing the redox stability of sodium cyanide ($NaCN^-$) in aqueous environments

This thermodynamic framework maps the stability fields of the dominant cyanide–bearing species as functions of redox potential and pH, thereby making the governing redox thresholds for interconversion explicit. The diagram also clarifies the leverage pH exerts on key equilibria and reactive intermediates: it shifts the HCN/CN- speciation via protonation control ($pK_a \approx 9.21$), shapes the generation and persistence of radical oxidants, and steers the accessible reaction channels. Operating near pH ≈ 10 is therefore not an arbitrary choice. In this window, hydroxyl – radical reactivity is favored while adverse outcomes are constrained, including radical recombination losses and HCN volatilization, which together improves the probability of directing CN^- toward selective oxidation into the less toxic CNO^- under controlled conditions. At the mechanistic level, $Na_2CO_3 \cdot 1.5H_2O_2$ dissociates in water to release hydrogen peroxide, which at pH 10:

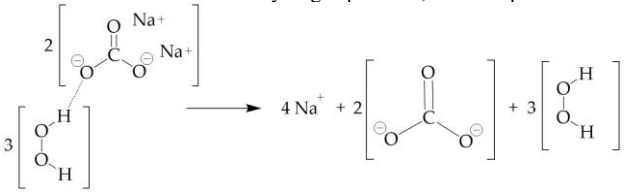

These radicals promote CN^- oxidation to CNO^- via coupled electron abstraction followed by nucleophilic addition, as expressed by:

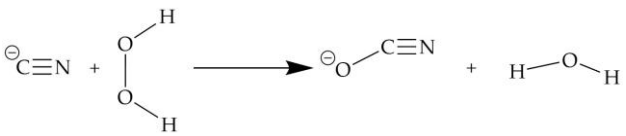

Oxidation of cyanide by sodium percarbonate derived $HO^\bullet$ is thermodynamically strongly favored ($\Delta G^0 \approx -177$ kJ mol^{-1}). The process performs best at pH ≈ 10, where HO_2^- predominates ($pK_a \approx 9.21$), a condition that supports high radical productivity while limiting back-recombination to H_2O_2. Shifting to pH 12 changes the chemistry: excess OH^- scavenges $HO^\bullet$ into less-reactive species, thereby suppressing the apparent kinetics and lowering the rate constant to ≈0.04 min^{-1}.

Parallel self-decomposition of H_2O_2 ($k \approx 0.001$-0.002 min^{-1} at pH 10-12), catalyzed by trace metals in the tailings, was negligible under optimized dosing conditions. Quantum calculations confirm a low-barrier transition state, supported by the high effective redox potential of HO• (1.8 V at pH 10), thereby ensuring fast kinetics in the initial phase.

Kinetics exhibit a clear biphasic pattern: a rapid radical-driven stage (first 40 min) limited by free cyanide availability, followed by a slower diffusion controlled phase caused by decreasing cyanide concentration, oxidant depletion, and reduced mixing efficiency at 300 rpm (**Fig. 4)**.

Semi logarithmic plots reveal an inflection at ~40 min and an apparent activation energy of ~18 kJ mol(20-25°C), characteristic of mass-transfer limitation. Low levels of Cu (4.74 mg/L), As (7.0 mg/L), and Fe (3.7 mg/L) exerted minimal interference, as $HO^\bullet$ retains high selectivity for CN^- over metal complexation [23] at these concentrations. The validated kinetic model, combined with response-surface-optimized reagent dosing, provides robust process control suitable for scale-up in continuous stirred-tank or agitated-tank systems used in industrial peroxide-based cyanide detoxification.

CONCLUSION

Sodium percarbonate allows cyanide-containing hydrometallurgical tailings to be treated in accordance with environmental requirements and consistently meets the ICMI criterion/limit of ≤0.2 mg/L free cyanide. The optimum determined by the response surface methodology for Altyntau Kokshetau tailings liquor is: pH 10, sodium percarbonate 3.5 g, 20-25 °C, mixing 300 rpm. In this mode, cyanide destruction shows a pronounced biphasic character: the initial rapid, radical-oxidation phase provides ~83% decomposition in the first 40 minutes, after which the process switches to a slower, diffusion-controlled regime that determines the required retention time (residence time). Therefore, maintaining an alkaline state at pH ≈10 is a controlling factor: it increases the stability of reactive oxidizing species and maintains a favorable cyanide specification; deviation from this window reduces the speed at the initial stage and prolongs the final stage of achieving compliance. After 8 h of retention, the total elimination rate exceeds 99.99%, with free cyanide dropping from 443.2 to 0.05 mg/L.

The mentioned kinetic regularities are directly translated into production recommendations. Implementation should be focused on a pH 10 setpoint and an optimal dose of percarbonate (3.5 g), and continuous mixing is provided to avoid mass transport restrictions and localized overdosing. Control of the free CN^- concentration should be carried out more often during the first hour, confirming the passage of the fast phase as expected; then the control interval is extended and the completion of the slow phase is checked. Since the accumulation of carbonate during processing can raise the pH of wastewater, the introduction of a post-oxidation neutralization unit and constant monitoring of pH/alkalinity should prevent deviations from the discharge requirements.

The catalyst-free, single-stage configuration and the working range defined by RSM simplify the design with respect to mixing and holding times, making scaling straightforward. However, for full validation, a pilot test is required: it must reproduce the actual hydrodynamics of the site, the coupling of solid particles and temperature variability.

According to laboratory estimates, the specific operating cost is US$ 0.7-1.0 per tonne of tailings; the bulk of it is determined by the percarbonate cost (~US$ 0.6 per tonne), with mixing energy and pH adjustment costs relatively insignificant. The main limitations are: switching to diffusion-restricted kinetics after the radical fast phase (which requires a long retention time) and the gradual accumulation of carbonate (which, if not controlled, can increase effluent pH).

Future work should focus on sustainability testing in the face of wider variability in waste composition (including high-load flows of cyanide and heavy metals), pilot demonstrations, evaluation of hybrid oxidizer schemes or continuous-flow reactor configurations to increase late-stage speeds, cost refinement based on operational data, and proving sustainable environmental safety through the formation of a long-term flow monitoring system.

Acknowledgements: This research is funded by the Science Committee of the Ministry of Science and Higher Education of the Republic of Kazakhstan (Grant № AP 23488663)

REFERENCES

1. Rajamanikandan R, Sasikumar K, Kosame S, Ju H: Nanomaterials, 13(2), 2023, 290. https://doi.org/10.3390/nano13020290
2. Eisler R, Wiemeyer SN: Reviews of Environmental Contamination and Toxicology, 183, 2004, 21–54. https://doi.org/10.1007/978-1-4419-9100-3_2
3. Koizhanova AK, Berkinbayeva AN, Sedelnikova GV, Kenzhaliyev BK, Azlan MN, Magomedov DR, Efremova YM: Metalurgija, 60(3–4), 2021, 423–426
4. Santanu P, Atanu P, Kumaresh G: Materials Chemistry Frontiers, 5(2), 2021, 584–602. https://doi.org/10.1039/d0qm00590
5. Kenzhaliyev B, Berkinbayeva A, Baltabekova Z, Moldabayeva G, Smailov K, Saulebekkyzy S, Tolegenova N, Karim D, Omirbek T: Processes, 13(4), 2025, 1099. https://doi.org/10.3390/pr13041099
6. Yessengaziyev A, Karshyga Z, Yersaiynova A, Tastanova A, Smailov K, Mukangaliyeva A, Orynbayev B: Metals, 15(10), 2025, 1133. https://doi.org/10.3390/met15101133
7. Antonini E, Brunori M, Rotilio GC, Greenwood C, Malmström BG: European Journal of Biochemistry, 23(2), 1971, 396–400. https://doi.org/10.1111/j.1432-1033.1971.tb01662
8. Koizhanova A, Kenzhaliyev B, Magomedov D, Kamalov E, Yerdenova M, Bakrayeva A, Abdyldayev N: ChemEngineering, 7(3), 2023, 54. https://doi.org/10.3390/chemengineering7030054
9. Brüger A, Fafilek G, Restrepo B OJ, Rojas-Mendoza L: Science of The Total Environment, 627, 2018, 1167–1173. https://doi.org/10.1016/j.scitotenv.2018.01.261
10. Zhang Y, Cui M, Wang J, Liu X, Lyu X: Minerals Engineering, 176, 2022, 107336. https://doi.org/10.1016/j.mineng.2021.107336
11. Liu Z, Guo X, Tian Q, Zhang L: Journal of Hazardous Materials, 440, 2022, 129778. https://doi.org/10.1016/j.jhazmat.2022.129778
12. Mooiman MB, Miller JD: Hydrometallurgy, 16(3), 1986, 245–261. https://doi.org/10.1016/0304-386X(86)90003-5
13. Johnson CA: Applied Geochemistry, 57, 2015, 194–205. https://doi.org/10.1016/j.apgeochem.2014.12.004
14. González-Valoys AC, Arrocha J, Monteza-Destro T, Vargas-Lombardo M, Esbrí JM, Garcia-Ordiales E, Jiménez-Ballesta R, García-Navarro FJ, Higueras P: Journal of Environmental Management, 302, 2022, 113979. https://doi.org/10.1016/j.jenvman.2021.113979
15. Kuyucak N, Akcil A: Minerals Engineering, 50–51, 2013, 13–29. https://doi.org/10.1016/j.mineng.2013.05.021
16. Anning C, Wang J, Chen P, Batmunkhi I, Lyu X: Waste Management & Research, 37(11), 2019, 1117–1126. https://doi.org/10.1177/0734242X19875528
17. Kenzhaliyev B, Surkova T, Yessimova D, Baltabekova Z, Abikak Y, Abdikerim B, Dosymbayeva Z: ChemEngineering, 7(1), 2023, 14. https://doi.org/10.3390/chemengineering7010014
18. Dong K, Xie F, Wang W, Chang Y, Lu D, Gu X, Chen C: Journal of Cleaner Production, 302, 2021, 126946. https://doi.org/10.1016/j.jclepro.2021.126946
19. Mamelkina MA, Herraiz-Carboné M, Cotillas S, Lacasa E, Sáez C, Tuunila R, Sillanpää M, Häkkinen A, Rodrigo MA: Separation and Purification Technology, 237, 2020, 116345. https://doi.org/10.1016/j.seppur.2019.116345
20. Kenzhaliyev B, Fischer D, Temirova S, Ultarakova A, Baltabekova Z, Bakhytuly N, Smailov K: Processes, 13(4), 2025, 997. https://doi.org/10.3390/pr13040997
21. Khodadad A, Teimoury P, Abdolahi M, Samiee A: Mine Water and the Environment, 27(1), 2008, 52–55. https://doi.org/10.1007/s10230-007-0021-5
22. Hai L, Fang X, Zhao X, Xu B, Cheng T: Scientific Reports, 13, 2023, 3831. https://doi.org/10.1038/s41598-023-30628-5
23. Chen X, Ren Y, Qu G, Wang Z, Yang Y, Ning P: Inorganic Chemistry Communications, 157, 2023, 111298. https://doi.org/10.1016/j.inoche.2023.111298
24. Berkinbayeva A, Kenzhaliyev B, Smailov K, Aimagambetov A, Kamenov B, Saulebekkyzy S, Tolegenova N, Putri PSR: Water Research X, 29, 2025, 100400. https://doi.org/10.1016/j.wroa.2024.100400
25. Kenzhaliyev B, Berkinbayeva A, Smailov K, Baltabekova Z, Saulebekkyzy S, Tolegenova N, Yessengaziyev A, Bakhytuly N, Tugambay S: Materials, 18(11), 2025, 2496. https://doi.org/10.3390/ma18112496
26. Xiong Q, Jiang S, Fang R, Liu S, Wu X: Journal of Hazardous Materials, 408, 2021, 124465. https://doi.org/10.1016/j.jhazmat.2020.124465
27. Luque-Almagro VM, Moreno-Vivián C, Roldán MD: Current Opinion in Biotechnology, 38, 2016, 9–13. https://doi.org/10.1016/j.copbio.2015.12.008
28. Uribe-Ramírez D, Cristiani-Urbina E, Morales-Barrera L: Microbiology Research, 15(1), 2024, 33–49. https://doi.org/10.3390/microbiolres15010003
29. Han W, Yang H, Tong L: Minerals, 13(5), 2023, 613. https://doi.org/10.3390/min13050613
30. Olaya-Abril A, Biełło K, Rodríguez-Caballero G, Cabello P, Sáez LP, Moreno-Vivián C, Luque-Almagro VM, Roldán MD: Microbial Biotechnology, 17(1), 2024, e14399
31. Petrov VF, Chepaikin EG, Bezrukov GM: RU Patent 2450979C2, 20 May 2012.
32. Taylor CJ, Pomberger A, Felton KC, Grainger R, Barecka M, Chamberlain TW, Bourne RA, Johnson CN, Lapkin AA: Chemical Reviews, 123(6), 2023, 3089–3126. https://doi.org/10.1021/acs.chemrev.2c00798
33. Kenzhaliyev B, Surkova T, Berkinbayeva A, Baltabekova Z, Smailov K, Abikak Y, Saulebekkyzy S, Tolegenova N, Omirbek T, Dosymbaeva Z: Metals, 15(3), 2025, 246. https://doi.org/10.3390/met15030246
34. Sukhatskiy Y, Znak ZO, Sozanskyi M, Shepida M, Gogate PR, Tsymbaliuk V: Chemistry and Chemical Technology, 18(2), 2024, 119–130. https://doi.org/10.23939/chcht18.02.119
35. Berkinbayeva A, Saulebekkyzy S, Kenzhaliyev B, Smailov K, Yessengaziyev A, Nurtazina N, Karim D, Birlikzhan Y: Metals, 15(10), 2025, 1162. https://doi.org/10.3390/met15101162

36. Vaca-Escobar K, Arregui-Almeida D, Espinoza-Montero P: npj Clean Water, 7, 2024, 103. https://doi.org/10.1038/s41545-024-00387-5
37. Jiang W, Lu Y, Feng Z, Yu H, Ma P, Zhu J, Wang Y, Sun J: Sustainability, 14, 2022, 15560. https://doi.org/10.3390/su142315560
38. Sokolovskaya L, Kvyatkovskiy S, Kozhakhmetov S, Semenova A, Sukurov B, Dyussebekova M, Shakhalov A: Minerals, 14(8), 2024, 781. https://doi.org/10.3390/min14080781
39. Ospanov YeA, Kvyatkovskiy SA, Kozhakhmetov SM, Sokolovskaya LV, Semenova AS, Dyussebekova M, Shakhalov AA: Canadian Metallurgical Quarterly, 2022. https://doi.org/10.1080/00084433.2022.2119495
40. Yessengaziyev A, Toishybek A, Mukangaliyeva A, Altaibayev B, Smailov K, Yersaiynova A, Abdyldayev N: Processes, 13(6), 2025, 1924. https://doi.org/10.3390/pr13061924
41. Kenzhaliyev B, Imankulov T, Mukhanbet A, Kvyatkovskiy S, Dyussebekova M, Tasmurzayev N: Metals, 15(2), 2025, 186. https://doi.org/10.3390/met15020186
42. Kenzhaliyev B, Koizhanova A, Fischer D, et al.: Transition Metal Chemistry, 2025. https://doi.org/10.1007/s11243-025-00637-7